Mol. Cells *31*, 39-48, January 31, 2011
DOI/10.1007/s10059-011-0002-1

Molecules and Cells

Abnormal Sperm Development in *pcd*^{3J}-/- Mice: the Importance of *Agtpbp1* in Spermatogenesis

Nameun Kim[1], Rui Xiao[1], Hojun Choi, Haiin Jo, Jin-Hoi Kim, Sang-Jun Uhm, and Chankyu Park*

Homozygous Purkinje cell degeneration (*pcd)* mutant males exhibit abnormal sperm development. Microscopic examination of the testes from *pcd*^{3J}-/- mice at postnatal days 12, 15, 18 and 60 revealed histological differences, in comparison to wild-type mice, which were evident by day 18. Greatly reduced numbers of spermatocytes and spermatids were found in the adult testes, and apoptotic cells were identified among the differentiating germ cells after day 15. Our immunohistological analysis using an anti-human AGTPBP1 antibody showed that AGTPBP1 was expressed in spermatogenic cells between late stage primary spermatocytes and round spermatids. A global gene expression analysis from the testes of *pcd*^{3J}-/- mice showed that expression of cyclin B3 and de-ubiquitinating enzymes USP2 and USP9y was altered by >1.5-fold compared to the expression levels in the wild-type. Our results suggest that the *pcd* mutant mice have defects in spermatogenesis that begin with the pachytene spermatocyte stage and continue through subsequent stages. Thus, *Agtpbp1*, the gene responsible for the *pcd* phenotype, plays an important role in spermatogenesis and is important for survival of germ cells at spermatocytes stage onward.

INTRODUCTION

Purkinje cell degeneration (*pcd*) mice display several interesting phenotypic abnormalities related to neuronal degeneration, including the degeneration of cerebellar Purkinje cells (Landis and Mullen, 1978; Mullen et al., 1976), retinal photoreceptor cells (Blanks et al., 1982; LaVail et al., 1982), mitral cells of the olfactory bulb (Greer and Shepherd, 1982), and certain thalamic neurons (O'Gorman, 1985; O'Gorman and Sidman, 1985). Ten different *pcd* alleles have been reported (www.informatics.jax.org) and a number of studies have been conducted to better understand the nature of the neuronal cell death in this model (Kyuhou and Gemba, 2005; Wang and Morgan, 2007; Wang et al., 2006). Although *pcd* mutants are known to lack the functional ATP/GTP binding protein 1 (*Agtpbp1*, also called *Nna1*) (Fernandez-Gonzalez et al., 2002), resulting in the *pcd* phenotype, the underlying mechanism linking the lack of this protein to the *pcd* phenotype is poorly understood.

In addition to the abnormal neuronal phenotype, *pcd* mutant mice have morphologically abnormal, including structural abnormalities of the head and tails from the electron microscopy, and significantly fewer mature sperm compared to wild-type mice (Handel and Dawson, 1981; Krulewski et al., 1989). However, detailed analysis on the initiation time of the defect, affected germ cell types and developmental reason for the abnormal sperm and testes has not been examined. We hypothesized that a similar mechanism might be responsible for both the neuronal and reproductive phenotypes. If true, a better understanding of the testicular phenotype of *pcd* mice may help elucidate the biological roles of *Agtpbp1* in sperm development, as well as neuronal survival.

Mammalian spermatogenesis can be divided into three principal phases: spermatogonial renewal and proliferation, meiosis, and spermiogenesis (Bellve et al., 1977). An abnormality in any one of these three processes can lead to a reduction in sperm count, as observed in male *pcd* mutant mice. To identify which of the phases of spermatogenesis is associated with abnormal spermatogenesis in *pcd* mutants, we performed a histopathological examination of postnatal and adult testes from *pcd*^{3J}-/- mice that carry a null allele due to a 12.2 kb deletion (Fernandez-Gonzalez et al., 2002). A global gene expression analysis was used to identify potential molecular mechanisms associated with abnormal spermatogenesis.

Here we showed that the significant reduction in sperm count in *pcd*^{3J}-/- mice was a result of the apoptotic death of spermatocytes and spermatids, indicating that *Agtpbp1* is important for spermatogenesis especially for the survival of germ cells at spermatocytes stage onward.

MATERIALS AND METHODS

Mice

Pcd^{3J} heterozygote (*pcd*^{3J}+/-) mice were purchased from the Jackson Laboratory (USA) and maintained under standard conditions (12-hour light/dark cycle) with food and water provided *ad libitum*. The animals used for these experiments were produced by crossing *pcd*^{3J} heterozygotes. The genotypes and phenotypes of the animals were determined as described in Xiao et al. (2005). The protocol for animal use was approved by the Institutional Animal Care and Use Committee (KU09066).

Department of Animal Biotechnology, Konkuk University, Seoul 143-701, Korea, [1]These authors contributed equally to this work.
*Correspondence: chankyu@konkuk.ac.kr

Received August 9, 2010; revised October 7, 2010; accepted October 11, 2010; published online November 23, 2010

Keywords: *Agtpbp1, apoptosis,* cyclin B3, meiosis, microarray, *Nna1, pcd, spermatogenesis,* testis, TUNEL

Sperm counts

Epididymides and testes were harvested from five-month-old mice following CO_2 euthanasia (n = 3). For sperm sampling, the cauda epididymis and vas deferens were cut with a surgical blade along the side of the corpus epididymis. The excised cauda epididymis was punctured and was compressed gently in phosphate-buffered saline (PBS) using the side of a 1 ml disposal syringe needle. Spermatozoa were diluted in PBS, washed three times by centrifugation at 300 × *g* for 5 min and placed into a hemacytometer. The number of sperm in five squares in the central grid of both sides of three hemacytometer chambers was counted per sample as described in Robb et al. (1978).

Histological analysis and immunohistological analysis

Mouse testes were dissected and fixed in 10% formalin overnight, rinsed with 70% ethanol, dehydrated in graded ethanol, and embedded in paraffin. Sections (5 μm) were cut and mounted on poly-L-lysine-coated glass slides. After de-paraffinization and hydration, sections were stained with hematoxylin and eosin for histological analysis. For immunohistological analysis, 6-μm thick sections were placed in 3% hydrogen peroxide for 30 min and sections were washed three times (5 min each) in PBS, blocked with normal sheep serum diluted in PBS (1:20). Sections were incubated with either anti-human AGTPBP1 (diluted 1:450, ProteinTech Group Inc, USA) or anti-mouse DDX4 (Abcam, USA) with blocking buffer, and standard avidin-biotin immunohistochemistry was performed with a rabbit ExtrAvidin® Peroxidase staining Kit (Sigma, Germany). Sections were visualized using DAB (3, 3′-diaminobenzidine Tablets, Sigma, Germany) and counterstained with Mayer's hematoxylin.

TUNEL staining

Sections (5 μm) were prepared as described above and mounted on poly-L-lysine-coated glass slides, followed by de-paraffinization and hydration. TUNEL reactions were performed with the In Situ Cell Death Detection Kit® (Roche, Switzerland) according to the manufacturer's protocol. Sections were counterstained with 4-6-diamidino-2-phenylindole (DAPI). Tubules containing TUNEL-positive cells were counted from three non-consecutive sections for each animal.

RT-PCR

Total RNA was isolated from testes using the Trizol reagent (Invitrogen, USA). Equal amounts of RNA were used for semi-quantitative RT-PCR. First strand cDNA was synthesized with 15mer random oligonucleotides (Promega, USA) and Superscript III reverse transcriptase (Invitrogen, USA). PCR reactions consisted of denaturation for 30 s at 94°C, annealing for 30 s at 55-59°C, and extension for 1 min at 72°C. The primer information for germ cell-specific markers and corresponding PCR conditions have been previously described (Choi et al., 2004). GAPDH was used as an internal standard. PCR products were run on 1.5% agarose gels, stained with ethidium bromide, and visualized by UV illumination. Each RT-PCR was performed at least three times from three different animals. The representative results were presented in Figures. Semi-quantitative analysis was performed with the BioDoc-Imaging System (UVP, UK). The expression intensity of genes was estimated with the ratio of the photodensity of the RT-PCR products of each gene and GAPDH. The average value was used for comparison. The primers used for the semi-quantitative RT-PCR to confirm the microarray results are described in Table 5.

Table 1. Sperm counts from wild-type and *pcd*^{3J}-/- mice

	Genotypes	
	+/+	*pcd*^{3J}-/-
Sperm count (mean ± SD)	$5.4 \pm 1.25 \times 10^8$	$4.15 \pm 0.58 \times 10^5$
Abnormal sperm (%)*	9.5 ± 6.54	91.1 ± 0.95

Five-month-old mice were used for the analysis.
*, Statistical difference, $P < 0.0005$

Microarray analysis

Three postnatal day 18 *pcd*^{3J}-/- mutant mice and three wild-type (*pcd*^{3J}+/+) littermates were used for the microarray analyses. Total RNA was isolated using RNeasy Mini Kit columns (Qiagen, Germany). RNA quality was assessed with an Agilent 2100 Bioanalyzer using an RNA 6000 Nano Chip (Agilent Technologies, Netherlands). Total RNA (300 ng) from each sample was converted to double-stranded cDNA using a random hexamer incorporating a T7 promoter. Amplified cRNA was generated from the double-stranded cDNA template through an *in vitro* transcription reaction, and was purified with the Affymetrix sample cleanup module (Affymetrix, US). cDNA was regenerated through random-primed reverse transcription, and was fragmented by uracil DNA glycosylase (UDG) and apurunic/apyrimidinic endonuclease 1 (APE 1) restriction endonucleases. cDNA was end-labeled in a terminal transferase reaction that incorporated a biotinylated dideoxynucleotide. Both cDNA and cRNA syntheses were performed according to the manufacturer's instructions (Affymetrix, US). Fragmented end-labeled cDNA was hybridized to the GeneChip® Mouse Gene 1.0 ST Arrays (Affimetrix), which contain 770,317 probes consisting of 25 mer length oligonucleotides, for 16 h at 45°C. After hybridization, the chips were stained and washed in a Genechip Fluidics Station 450 (Affymetrix) and scanned using a Genechip Array Scanner 3000 7G (Affymetrix). Expression data were normalized and log2 transformed using the robust multichip average (RMA) method implemented in the Bioconductor package RMA (Bolstad et al., 2003; Irizarry et al., 2003). Two-tailed, unpaired Student's *t*-tests were used as a statistical method for the selection of differentially expressed genes.

RESULTS

Decreased sperm numbers and testicular atrophy in *pcd*^{3J}-/- mice

Spermatozoa were collected from the epididymis and vas deferens of 5-month-old *pcd*^{3J}-/- mice and wild-type littermates and counted. Sperm counts in *pcd*$^{3J-/-}$ mice were significantly lower (approximately 1000 fold) than their wild-type littermates (Table 1). In addition to having significantly lower sperm counts, approximately 91% of the spermatozoa in the *pcd*^{3J}-/- mice exhibited severely malformed heads and crenulated tails compared to those observed in the wild-type mice (Figs. 1A and 1B). Histological analysis of the cauda epididymis from *pcd*^{3J}-/- mice showed that few sperm were present in the cauda epididymis (Figs. 1C and 1D). Testicular size was similar between wild-type and *pcd*^{3J}-/- mice at 8 weeks, in spite of the significantly lower sperm counts in the *pcd*^{3J}-/- mice. However, at 20 weeks, the testes of the *pcd*^{3J}-/- mice were much smaller than those of the control wild-type littermates, suggesting that spermatogenic abnormalities worsened over time (Fig. 2).

Aberrant spermatogenesis in *pcd*^{3J}-/- mice

In order to identify the underlying cause of the lower sperm

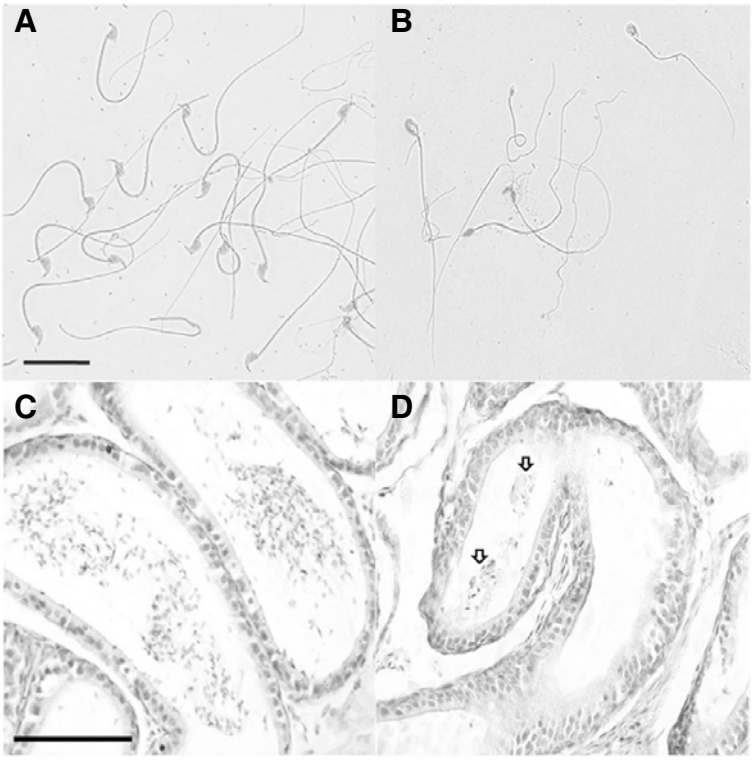

Fig. 1. Histological analysis of cauda epididymis and abnormally shaped testicular spermatozoa in 5-month-old *pcd*^{3J}-/- mice. Spermatozoa from wild-type littermates (A) and from *pcd*^{3J}-/- mice (B) with severely malformed heads and disorganized tails of uneven thickness. The cauda epididymis from *pcd*^{3J}-/- mice (D) contained few sperm compared to the wild-type controls (C). Scale bars: 20 μm in panels A and B; 100 μm in panels C and D.

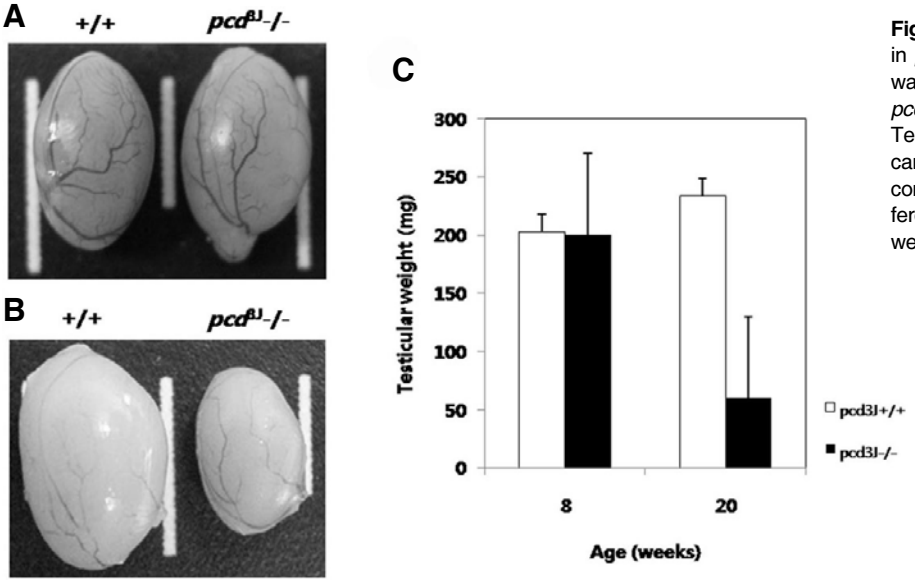

Fig. 2. Development of testicular atrophy in *pcd*^{3J}-/- mice (n = 3). (A) Testicular size was similar between wild-type (left) and *pcd*^{3J}-/- (right) mice at 8 weeks of age. (B) Testes from *pcd*^{3J}-/- mice (right) are significantly smaller than those from wild-type controls (left) at 20 weeks of age. (C) Differences in testicular weights at 8 and 20 weeks of age (n = 3).

counts in the *pcd*^{3J}-/- mice, we analyzed the phenotypes of cells in the seminiferous tubules in 60-day-old adult *pcd*^{3J}-/- mice. The majority of the seminiferous tubules in the *pcd*^{3J}-/- mice contained only a few spermatozoa-like cells with distinctive elongated nuclei (Figs. 3A-3D). Cells located adjacent to the basal lamina at the edge of the seminiferous tubules were not different in appearance from those in wild-type mice, suggesting that the *pcd*^{3J}-/- mutation does not affect the population of spermatogonia (Table 2). The most obvious difference between the seminiferous tubules of wild-type and *pcd*^{3J}-/- mice was the degeneration of cells in the meiotic phase and the subsequent reduction in the number of spermatids in the *pcd*^{3J}-/- mice. Pachytene spermatocytes, round spermatids, and elongated spermatids were present in the *pcd*^{3J}-/- mice, but the numbers of these cells were notably lower than found in the wild-type mice (Figs. 3C and 3D). Multinucleated cells or cell aggregates, which appeared to be haploid cells, were also observed in a degenerated state in the luminal center of the seminiferous tubules (Figs. 3E and 3F).

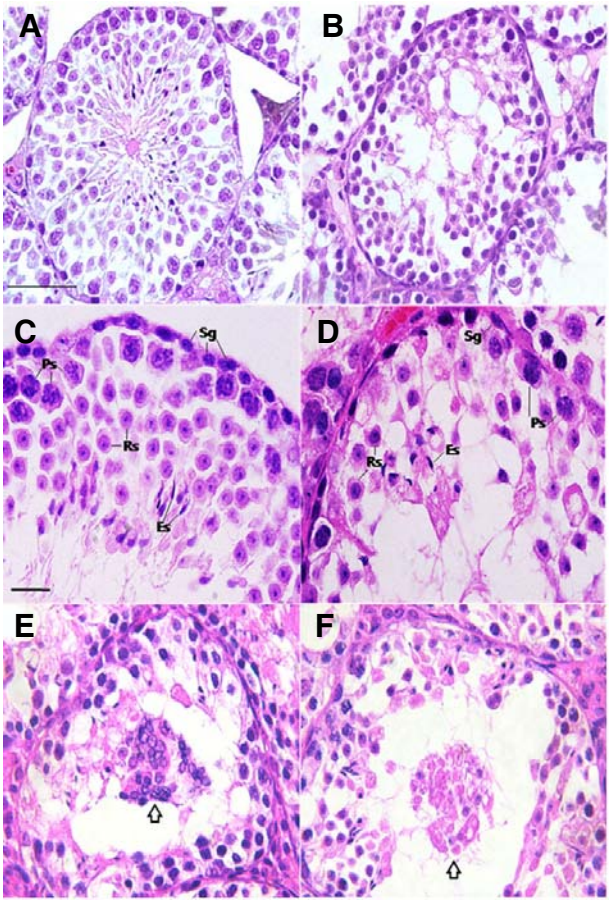

Fig. 3. Histological analysis of testes from adult *pcd*^{3J}-/- mice. The testicular sections of wild-type (A, C) and *pcd*^{3J}-/- (B, D, E and F) mice at postnatal day 60 were stained with hematoxylin and eosin. (A, B) there are significantly fewer differentiating male germ cells in *pcd*^{3J}-/- mice compared to wild-type controls. (C, D) pachytene spermatocytes, round spermatids and elongated spermatids were present, but in significantly lower numbers in testes from *pcd*^{3J}-/- mice compared to wild-type controls (Sg, spermatogonia; Ps, pachytene spermatocyte; Rs, round spermatid; Es, elongated spermatid). (E, F) Aggregated haploid cells (arrows) are present and appear to be degenerating within the lumen of the seminiferous tubules of *pcd*^{3J}-/- mice. Scale bars: 100 μm in (A, B) 20 μm in (C-F).

Table 2. Comparison of germ cell numbers in the stage VI seminiferous tubules between wild-type and *pcd*^{3J}-/- testes

Cell types	Cell number (mean ± SD)	
	+/+	*pcd*^{3J}-/-
Spermatogonia	20 ± 6.66	19.5 ± 4.07
Spermatocyte	51 ± 19	17 ± 6*
Round spermatid	86 ± 6	21 ± 5*

The stages of seminiferous tubules were distinguished as described by Ahmed et al. (2009). The values indicate germ cell numbers for each cell type per seminiferous tubule. Three stage VI tubules, which were most easily identifiable in our experiment, were counted from each testis. Three mice at the age of day 60 were analyzed.
*, Statistical difference, P < 0.05

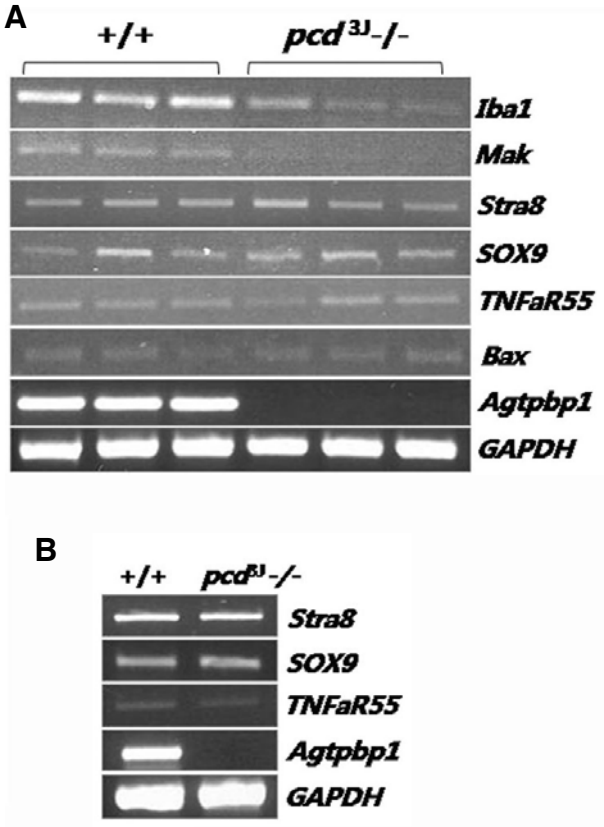

Fig. 4. Analysis of male germ cell-specific gene expression in the testes of *pcd*^{3J}-/- mice using semi-quantitative RT-PCR. (A) Gene expression in adult testes. Only haploid specific markers exhibited decreased expression levels. (B) Gene expression in testes at postnatal day 18. There were no differences between *pcd*^{3J}-/- mice and wild-type controls. Marker descriptions: Iba 1, haploid-specific; Mak, type B spermatogonia- and early spermatocyte-specific; Stra8, type A spermatogonia-specific; SOX9, Sertoli cell-specific; TNFaR55, Leydig cell and Sertoli cell-specific; Bax, a proapoptotic protein in the caspase dependent pathway. GAPDH was used as a control for the amount of cDNA used in the PCR reactions. *Agtpbp1* expression was virtually undetectable in samples from *pcd*^{3J}-/- mice.

Decreased expression levels of haploid specific genes in the testes of *pcd*^{3J}-/- mice

Semi-quantitative RT-PCR of male germ cell-specific markers was used to identify the affected cell populations in the testes of *pcd*^{3J}-/- mice. There were no differences in the expression of Stra8, a marker specific to type A and B spermatogonia and pre- and early leptotene spermatocytes (Nguyen et al., 2002), in testes from wild-type and *pcd*^{3J}-/- mice. However, the expression of a meiotic germ cell-specific marker, Mak, and a haploid-specific marker, Iba1, was much lower in testes from *pcd*^{3J}-/- mice (Fig. 4A), which is consistent with the histological analysis. There was no difference in Bax expression in testes from wild-type and *pcd*^{3J}-/- mice, suggesting that the cell death observed in *pcd*^{3J}-/- mice was not initiated by *Bax* expression. The *TNFaR55* and *Sox9* expression patterns indicated that the abnormalities were not due to an absence of either Leydig or Sertoli cells. Using the same cell-specific markers, there were no differences in gene expression in testes from pre-pubertal (postnatal day 18) wild-type and *pcd*^{3J}-/- mice (Fig. 4B), suggesting that degeneration is specific to male germ cells and not

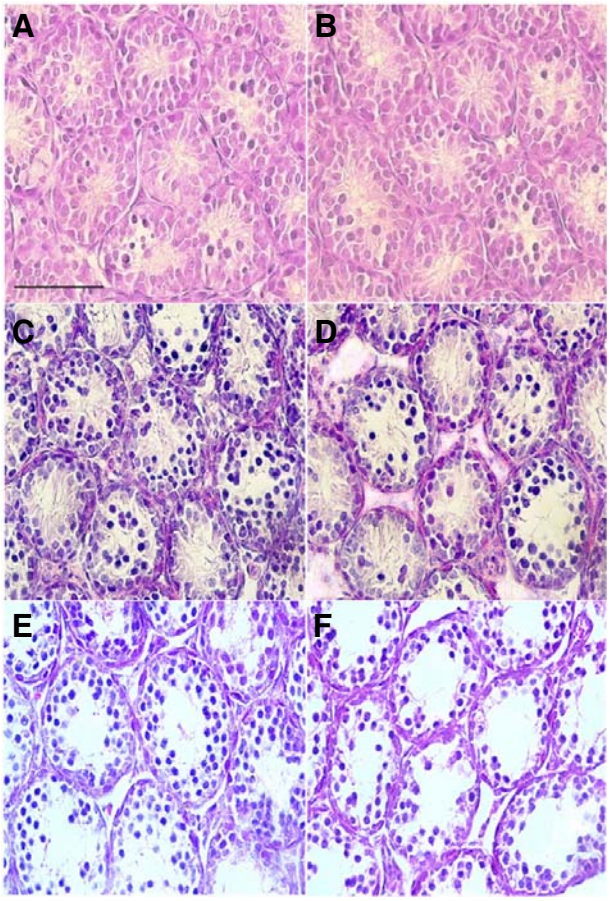

Fig. 5. Histological analysis of postnatal testicular development in *pcd*^{3J}-/- mice. Representative histological sections of testes from wild-type (A, C, and E) and *pcd*^{3J}-/- mice (B, D, and F) at postnatal days 12 (A, B), 15 (C, D) and 18 (E, F) stained with hematoxylin and eosin. Tissue from three animals was analyzed at each developmental stage. A decrease in the number of germ cells within the seminiferous tubules of the *pcd*^{3J}-/- mice was apparent at postnatal day 18 (E, F). Scale bars: 100 μm.

somatic cells.

Temporal analysis of testicular development in pre-pubertal testes of *pcd*^{3J}-/- mice

Histological analyses of testes at postnatal days 12, 15 and 18 were performed to determine the developmental onset of germ cell abnormalities in the *pcd*^{3J}-/- mice (Fig. 5). An obvious difference was recognizable at postnatal day 18, by which time the number of cells within the seminiferous tubules was decreased. Direct cell counting from hematoxylin and eosin-stained testicular sections from postnatal day 18 mice showed that, in the *pcd*^{3J}-/- mice, there were 34% fewer cells within the seminiferous tubules compared to wild-type mice (Table 3). There were no significant differences in the number of cells within the seminiferous tubules at postnatal days 12 and 15 between wild-type and *pcd*^{3J}-/- mice.

Apoptotic cell death during spermatogenesis in the testes of *pcd*^{3J}-/- mice

Histological sections of testes from *pcd*^{3J}-/- mice at postnatal days 12, 15 and 18, as well as at 4 months of age, were examined for evidence of apoptosis using terminal deoxynucleotidyl transferase-mediated deoxyuridinetriphosphate nick end-labeling (TUNEL) staining. TUNEL-positive signals were identified in testes at postnatal day 15 and the percentage of TUNEL-positive tubules increased with age (Table 4). Approximately 52% of the tubules from the *pcd*^{3J}-/- mice contained at least one apoptotic cell at 4 months of age. In mice, spermatogenesis (differentiation of primitive type A spermatogonia to type A and type B spermatogonia) begins at postnatal day 8, followed by the initial appearance of leptotene, zygotene, and pachytene spermatocytes at days 10, 12, and 14, respectively. At day 18, secondary spermatocytes and round spermatids appear (Bellve et al., 1977). The absence of a TUNEL-positive signal at day 12 and the presence of a TUNEL-positive signal at day 15 (Figs. 6A and 6B) suggests that apoptosis begins with the pachytene spermatocytes and that the early periods of spermatogenesis are not affected in *pcd*^{3J}-/- mice. Some of the apoptotic cells appeared to be pachytene spermatocytes or spermatids based on their morphology and location within the seminiferous tubule (Figs. 6D-6F), suggesting that apoptosis in the testes of *pcd*^{3J}-/- mice is not cell type-specific.

Table 3. Temporal comparison of the number of germ cells in the seminiferous tubules of wild-type and *pcd*^{3J}-/- mice

Genotype	Age (day)	Number of germ cells (mean ± SD)
+/+	12	37 ± 4.24
pcd^{3J}-/-		36.7 ± 3.09
+/+	15	40.7 ± 3.09
pcd^{3J}-/-		41 ± 1.41
+/+	18*	51 ± 2.16
pcd^{3J}-/-		33.7 ± 4.92

For germ cell counting, all cells with clear nuclei within the tubule except for Sertoli cells were counted. The cell numbers indicate a total number of germ cells in a seminiferous tubule which resulted from counting three tubules per testis. Three mice were analyzed.
*, Statistical difference, P < 0.005

Table 4. Frequency of TUNEL-positive seminiferous tubules in wild-type and *pcd*^{3J}-/- mice

Genotype	Age (day)	TUNEL positive tubule (%) (mean ± SD)
+/+	12	0.58 ± 0.19
pcd^{3J}-/-		0.61 ± 0.2
+/+	15*	1.56 ± 0.36
pcd^{3J}-/-		13.96 ± 1.47
+/+	18*	2.28 ± 0.33
pcd^{3J}-/-		18.81 ± 2.68
+/+	120*	3.85 ± 1.01
pcd^{3J}-/-		53.26 ± 1.24

*, Statistical difference, P < 0.005

Analysis of AGTPBP1 expression during testicular development by immunohistological analysis

We analyzed the expression of AGTPBP1 protein in normal mouse testes using an anti-human AGTPBP1 antibody to evaluate the primary origin of the testicular phenotypes of *pcd*^{3J}

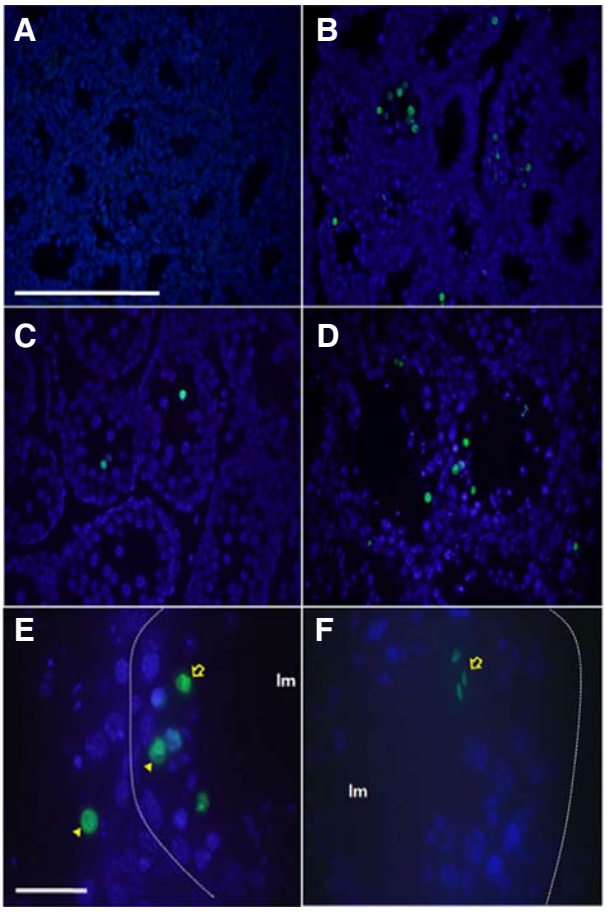

Fig. 6. Identification of apoptotic cells in the testes of *pcd*^{3J}-/- mice during spermatogenesis using TUNEL staining. Representative TUNEL reactions from the testicular sections of three *pcd*^{3J}-/- mice at postnatal days 12 (A), 15 (B) and 18 (C), and at 4 months of age (D-F). TUNEL-positive cells are indicated in green and counter-stained with DAPI. (A) Lack of apoptotic signals at postnatal day 12. (B-D) An increase in apoptotic-positive cells from postnatal day 15 onwards. (E) A higher magnification of the seminiferous tubule reveals TUNEL-positive signals in pachytene spermatocytes (arrowhead) and round spermatids (arrow). The position of the basal lamina is indicated by the dotted lines. The lumen is indicated by lm. (F) TUNEL-positive elongated spermatids (arrow). Most of cells from the wild type TUNEL positive control experiment were TUNEL positive (data not shown). Scale bars: 100 μm in (A-D) and 20 μm in (E, F).

-/- mice. Immunohistochemical analysis of 4-month-old adult testes showed that the number of AGTPBP1 expressing cells was much higher compared to the developing testes (Fig. 7). AGTPBP1 expression was almost undetectable in testes at days 12 and 15 (data not shown), but clearly detectable at day 18 (Fig. 7B), which corresponded precisely to the appearance of histological differences between wild-type and *pcd*^{3J}-/- testes at postnatal day 18 (Fig. 5). The AGTPBP1 antibody positive cells at day 18 were most likely to be late stage primary spermatocytes according to the appearance of spermatogenic cells in the prepuberal mouse testis (Bellve et al., 1977). Therefore, the antibody positive cells in the 4 month adult testis were likely to be germ cells between late stage primary spermatocytes and round spermatids, since most of elongated spermatids were

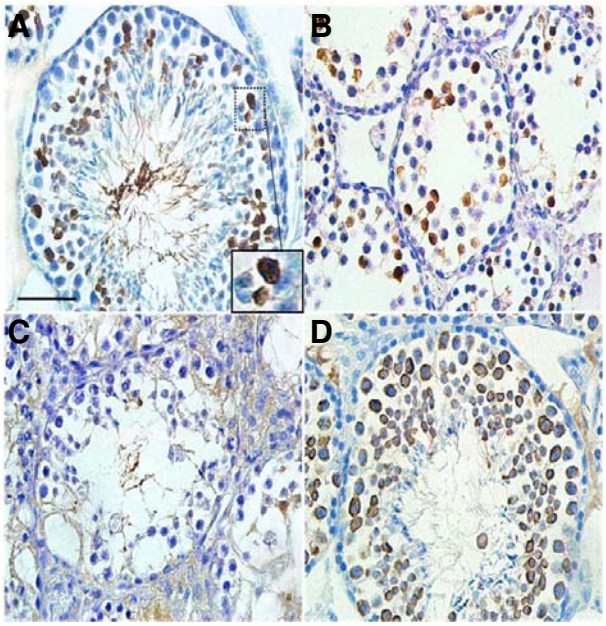

Fig. 7. Immunohistochemical localization of AGTPBP1 in mouse testes. Testes sections from wild-type (A, B) and *pcd*^{3J}-/- (C) mice at 4 months of age (A) or at postnatal day 18 (B) were stained with a human anti-AGTPBP antibody. (A) Germ cells between late stage primary spermatocytes and round spermatids were positive for the antibody staining. The image within the large square is the enlarged image of the small square, indicating the staining of pachytene spermatocytes. (B) Late stage spermatocytes were positive for the antibody. (C) No clear expression of AGTPBP1 was observed. (D) In the wild type testis, all spermatogenic cells from the spermatocyte to round spermatid stages were stained by the anti-MVH antibody as a positive control for developing germ cells. Scale bars, 100 μm for (A-D).

free of AGTPBP1 antibody staining. These results suggest that the presence of male germ cell abnormalities in *pcd*^{3J}-/- mice is a cell autonomous phenomenon rather than being indirectly caused by abnormal functioning of somatic cells, such as Sertoli cells, as suggested by the semi-quantitative RT-PCR of male germ cell-specific genes in Fig. 4.

Up-regulation of cyclin B3 in the testes of *pcd*^{3J}-/- mice

Findings from gene expression studies can help identify relevant biological pathways. RNA isolated from three pairs of testes from wild-type and *pcd*^{3J}-/- mice at postnatal day 18 was subjected to a genome-scale gene expression analysis using the Affymetrix GeneChip Mouse Gene 1.0 ST Array, which includes approximately 28,000 genes. RNA from postnatal day 18 was used to minimize the changes in gene expression that might occur in response to pathological changes in the *pcd*^{3J}-/- mice, because postnatal day 18 was the earliest time point at which structural differences between testes from wild-type and *pcd*^{3J}-/- mice were observed via histopathology. Spearman rank correlation coefficients between any pairwise comparisons from the six sets of array data ranged from 0.986 to 0.992, indicating reliable results.

Results from three wild-type and three *pcd*^{3J}-/- mice were averaged and examined for genes that were differentially expressed. Differences in gene expression patterns between the wild-type and *pcd*^{3J}-/- mice were much smaller than expected

Table 5. Primers and parameters used in semi-quantitative RT-PCR experiments to confirm the results of the microarray analysis

Gene (Acc No.)	Primer sequences	Annealing temp. (No. of cycles)	Product size (bp)
Ccnb3 (NM_183015)	5′-CTACTGAGGAACCATCTGTC-3′ 5′-GTGAGCGTCACCTTCCTAAT-3′	53 (23)	280
Usp9Y (NM_148943)	5′-TGTGAGGAATCCAGAGTTG-3′ 5′-CTCTTCTTCATGCTGTGGTG-3′	56 (27)	283
Agtpbp1 (NM_023328)	5′-AACGTCAGGAGAGCGGTGGA-3′ 5′-AGAATTTTCATCCCATTCGC-3′	56 (29)	188
Rabl4 (NM_025931)	5′-TCTCCGCTAGTACCTGGTTA-3′ 5′-GAACTGGCACTGTCTTCAC-3′	58 (25)	177
Cds1 (NM_173370)	5′-CAAGATGGAAGAACTGGtGG-3′ 5′-TGGTAGCGAATGAGGAACTG-3′	58 (25)	307
GAPDH	5′-CTCACTCAAGATTGTCAGCA-3′ 5′-GTCATCATACTTGGCAGGTT-3′	57 (27)	346

Table 6. Genes with expression differences >1.5 fold in the testes of *pcd*^{3J}-/- mice compared to wild-type controls

Gene symbol	GenBank accession No.	Gene description	Fold differences
Ccnb3	NM_183015	Cyclin B3	+1.67
Usp9y	NM_148943	Ubiquitin specific peptidase 9, Y chromosome	+1.66
Zfy1	NM_009570	Zinc finger protein 1, Y linked	+1.56
Zim1	NM_011769	Zinc finger, imprinted 1	+1.54
Zfy2	NM_009571	Zinc finger protein 2, Y linked	+1.54
Pet2	NM_008821	Plasmacytoma expressed transcript 2	+1.54
Gm650	XM_911239	Gene model 650, (NCBI)	+1.54
Agtpbp1	NM_023328	ATP/GTP binding protein 1	-1.51
Bscl2	NM_008144	Bernardinelli-Seip congenital lipodystrophy 2 homolog (human)	-1.51
Ttc30a1	NM_030188	Tetratricopeptide repeat domain 30A1	-1.53
Usp2	NM_198092	Ubiquitin specific peptidase 2	-1.54
Rabl4	NM_025931	RAB, member of RAS oncogene family-like 4	-1.56
Cds1	NM_173370	CDP-diacylglycerol synthase 1	-1.57
Mgll	NM_011844	Monoglyceride lipase	-1.63
Aqp9	NM_022026	Aquaporin 9	-1.65
Zfa	NM_009540	Zinc finger protein, autosomal	-1.70
Lcn5	NM_007947	Lipocalin 5	-1.78
Insl6	NM_013754	Insulin-like 6	-1.92
ENSMUSG00000073430	ENSMUST00000097363 (ENSEMBL)	Predicted gene, ENSMUSG00000073430	-2.04
Ces7	NM_001003951	Carboxylesterase 7	-2.82

(ArrayExpress accession, E-MEXP-2570). There were 20 genes that exhibited differences in expression levels, defined by a >1.5-fold change and statistical significance at the $p < 0.5$ level. Seven genes were up-regulated and 13 genes were down-regulated in the testes of the *pcd*^{3J}-/- mice compared to wild-type controls (Table 6). The results of individual comparisons of the expression levels of these 20 genes, from each of the three independent experiments, were consistent with the results of the paired comparisons of the averaged values.

Among the genes that were differentially expressed, *Ccnb3* (cyclin B3), *Usp9y* (ubiquitin-specific peptidase 9 Y chromosome), *Zfy1* (zinc finger protein 1, Y-linked), *Zfy2* (zinc finger protein 2, Y-linked), and *Insl6* (insulin-like 6) are directly involved in germ cell development (Lee et al., 2003; Lok et al., 2000; Nagamine et al., 1990; Refik-Rogers et al., 2006; Zambrowicz et al., 1994). Interestingly, the meiosis-related cyclin *Ccnb3* (McCleland et al., 2009) was up-regulated in the testes of *pcd*^{3J}-/- mice. Results of the microarray analysis were confirmed using semi-quantitative RT-PCR for five genes that are functionally relevant to the *pcd* phenotype (Fig. 8). Results from the semi-quantitative RT-PCR experiments were consistent with the microarray data, although there was some variation in the degree of expression measured by the two methods.

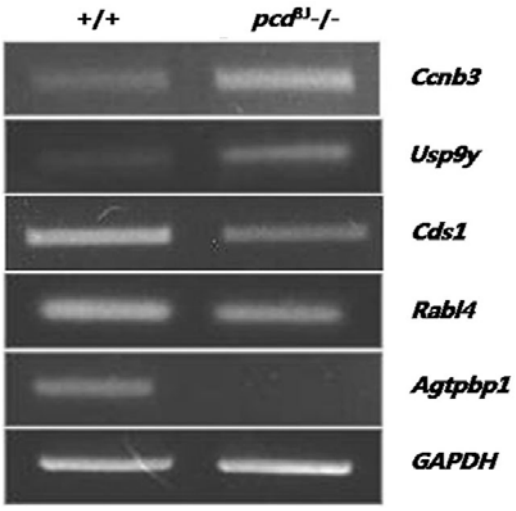

Fig. 8. Confirmation of the results from the microarray analysis by semi-quantitative RT-PCR. Three independent experiments using three pairs of wild-type and *pcd*^{3J}-/- animals showed similar results. GAPDH was used as a control for the amount of cDNA used in the PCR reactions.

DISCUSSION

Apoptotic cell death is a common phenotype associated with mutations of *Agtpbp1*

Neuronal degeneration is considered to be the primary phenotype of *pcd*^{3J}-/- mice. Although *pcd*^{3J}-/- mutant mice were shown to exhibit lower sperm counts and abnormal sperm development compared to wild-type animals, a detailed examination of the abnormal testicular phenotype of *pcd*^{3J}-/- mice has not been performed. The results presented here show that apoptosis is responsible for the degeneration of male germ cells during spermatogenesis in the testes of *pcd*^{3J}-/- mice, suggesting that *Agtpbp1* may represent a common mechanism underlying cell survival or maintenance in different tissues (i.e., neuronal and testicular tissues). The degeneration of germ cells in the testes begins around postnatal day 15, which is similar to the time at which Purkinje cells begin to die in the brain (Landis and Mullen, 1978; Mullen et al., 1976).

The presence of abnormalities in male germ cell development in *pcd*^{3J}-/- mice prompted an examination of female germ cell development or folliculogenesis, which was conducted by comparing the histological structures of adult ovaries in female *pcd*^{3J}-/- and wild-type mice. However, there were no significant differences between the number of follicles in female *pcd*^{3J}-/- and wild-type mice (data not shown), which is consistent with the lack of *Agtpbp1* expression in the adult mouse ovary (Harris et al., 2000). Since our result suggest an important role of Agtpbp1 during male germ cells differentiation, the understanding of underlying molecular mechanisms may reveal unidentified cellular interactions which are required for the differentiation of male germ cells.

The function of *Agtpbp1* in spermatogenesis

Studies using genetically-modified mice have played an important role in enhancing our understanding of spermatogenesis (reviewed by Cooke and Saunders, 2002; de Rooij and de Boer, 2003). Results from these studies suggest that *pcd*^{3J}-/- mice can be used as a model to study detailed molecular mechanisms of spermatogenesis and male meiosis.

Spermatogenic abnormalities can be caused by a disruption of the meiotic cell cycle or of germ cell differentiation. A disruption of the cell cycle during meiosis will typically result in cell cycle arrest and apoptosis. For example, a targeted disruption of cyclin A1 in mice has been shown to block spermatogenesis before the first meiotic division (Liu et al., 1998). However, a disruption of germ cell differentiating factors tends to result in successive decreases in differentiating germ cells, manifested by low sperm counts or structural abnormalities in spermatozoa over time. For example, mice deficient in huntingtin interacting protein 1 (HIP1) exhibited low sperm counts and abnormally shaped spermatids (Khatchadourian et al., 2007).

In this study, apoptotic cell death in *pcd*^{3J}-/- mice first appeared in pachytene spermatocytes without a stage-specific peak in apoptosis. Although the number of germ cells in *pcd*^{3J}-/- mice was significantly lower than those in wild-type controls, germ cells in latter stages were present. Taken together, these findings suggest that the testicular phenotype of *pcd*^{3J}-/- mice might be a result of abnormal germ cell differentiation. However, the possibility that a failure in cell cycle control during meiosis played a causal role cannot be ruled out in light of the altered expression of *Ccnb3* in the testes of *pcd*^{3J}-/- mice. Therefore, these results suggest that the absence of *Agtpbp1* may affect meiotic cell cycle control and subsequent spermiogenesis.

In addition to autonomous germ cell defects, endocrine abnormality such as testosterone or LH deficiency also lead to the hypogonadism and failure in spermatogenesis. However, no detailed study on the endocrine system integrity of *pcd* mutant mice has been reported. In testosterone deficient mice, spermatogenesis does not progress beyond the pachytene stage (O'Shaughnessy et al., 2010). LH deficiency also leads to failure in the proper development of testes in males and female reproductive organs (Ma et al., 2004). In *pcd* mutant mice, the distribution of testosterone receptors is similar to that of normal mice (Fox et al., 1977). Furthermore, *pcd* mutant testes produce spermatids which are the more progressed stage of male germ cells than expected from mice with testosterone or LH deficiency regardless of their morphological abnormality. In females, *pcd* mutants are fertile (Mullen et al., 1976) and their ovarian function is normal based on our histological analysis (data not shown). Therefore, it is less likely that the phenotypes of *pcd* mutant mice directly arise from endocrine defects.

Interpretation of DNA microarray analysis

Four previous studies, including one from our laboratory, have used microarray analyses to examine gene expression in cerebellar tissues at different stages of development (Ford et al., 2008; Rong et al., 2004; Sun et al., 2006; Xiao et al., 2005). There have been some discrepancies between these studies in the expression of different genes. However, many of the apparent discrepancies between previous studies may be the result of analyses that were conducted during different developmental stages.

Here, we report the first gene expression profile of the testes of *pcd*^{3J}-/- mice. The genome-level gene expression profile at postnatal day 18 provides new insights into the possible mechanisms of testicular development and spermatogenesis in *pcd*^{3J}-/- mice. Ubiquitin-dependent proteolysis is an important mechanism for controlling spermatogenesis and sperm quality (Sutovsky, 2003). Cyclins are substrates of ubiquitinating enzymes (Zachariae et al., 1998). Therefore, the altered expression of two de-ubiquitinating enzymes, Usp9y and Usp2, together with the up-regulation of *Ccnb3* in the testes of *pcd*^{3J}-/- mice suggests that ubiquitin-based proteolysis may be involved

in testicular development and spermatogenesis.

Consistent with a previous study in which CDP-diacylglycerol synthase 1 (*Cds1*) was down-regulated in the cerebella of 4-month-old *pcd*^{3J}-/- mice (Rong et al., 2004), *Cds1* was also down-regulated in the testes of *pcd*^{3J}-/- mice in this study. *Cds1* is also involved in the light-induced degeneration of retinal photoreceptors in *Drosophila* (Wu et al., 1995). Thus, evidence from gene expression studies suggests that there are common factors involved in the degeneration of Purkinje cells, male germ cells, and retinal photoreceptors.

Possible interactions between *Ccnb3* and *Agtpbp1*

Microarray analysis of gene expression showed that expression of *Ccnb3* was increased in the testes of *pcd*^{3J}-/- mice compared to wild-type controls, suggesting that there could be a possible interaction between *Agtpbp1* and *Ccnb3*. *Ccnb3* is a meiosis-related cyclin that is expressed from the leptotene and zygotene stages through to the end of the pachytene stage. However, it can also be interpreted that the increased *Ccnb3* expression level at day 18 may just arise from relative enrichment of *Ccnb3* expressing cells at day 18 in the mutant testis since the day 18 testis already contains 34% less germ cells than that of wild type (Table 3).

Prolonged expression of *Ccnb3* in transgenic mice leads to a marked disruption in spermatogenesis (Refik-Rogers et al., 2006). The testicular phenotype of *Ccnb3* transgenic mice was surprisingly similar to the testicular phenotype of *pcd*^{3J}-/- mice, which may suggests that CCNB3 interacts with AGTPBP1. Although the precise function of AGTPBP1 remains unknown, recent reports have suggested that it may be a member of the carboxypeptidase family (Harris et al., 2000; Kalinina et al., 2007; Rodriguez de la Vega et al., 2007). If AGTPBP1 indeed functions as a cytosolic carboxypeptidase (CCP), there should be corresponding target substrate proteins. It may be interesting to examine whether an enzyme-substrate relationship exists between AGTPBP1 and CCNB3.

ACKNOWLEDGMENTS

This work was supported by a grant from the Technology Development Program for Agriculture and Forestry, Ministry for Agriculture, Forestry and Fisheries, and a grant from the Biogreen 21 Program (grant number 20070401-034-029-01), Rural Development Administration, Republic of Korea. Rui Xiao was supported by the 2009 KU Brain Pool Program of Konkuk University, Korea.

REFERENCES

Ahmed, E.A., and de Rooij, D.G. (2009). Staging of mouse seminiferous tubule cross-sections. Methods Mol. Biol. *558*, 263-277.

Bellve, A.R., Cavincchia, J.C., Millette, C.F., O'Brien, D.A., Bhatnogar, Y.M., and Dym, M. (1977). Spermatogenic cells of the prepuberal mouse. Isolation and morphological characterization. J. Cell Biol. *74*, 68-85.

Blanks, J.C., Mullen, R.J., and LaVail, M.M. (1982). Retinal degeneration in the pcd cerebellar mutant mouse. II. Electron microscopic analysis. J. Comp. Neurol. *212*, 231-246.

Bolstad, B.M., Irizarry, R.A., Astrand, M., and Speed, T.P. (2003). A comparison of normalization methods for high density oligonucleotide array data based on variance and bias. Bioinformatics *19*, 185-193.

Choi, Y.J., Ok, D.W., Kwon, D.N., Chung, J.I., Kim, H.C., Yeo, S.M., Kim, T., Seo, H.G., and Kim, J.H. (2004). Murine male germ cell apoptosis induced by busulfan treatment correlates with loss of c-kit-expression in a Fas/FasL-and p53-independent manner. FEBS Lett. *575*, 41-51.

Cooke, H.J., and Saunders, P.T. (2002). Mouse models of male infertility. Nat. Rev. Genet. *3*, 790-801.

De Rooij, D.G., and de Boer, P. (2003). Specific arrests of spermatogenesis in genetically modified and mutant mice. Cytogenet. Genome Res. *103*, 267-276.

Fernandez-Gonzalez, A., La Spada, A.R., Treadaway, J., Higdon, J.C., Harris, B.S., Sidman, R.L., Morgan, J.I., and Zuo, J. (2002). Purkinje cell degeneration (pcd) phenotypes caused by mutations in the axotomy-induced gene, Nna1. Science *295*, 1904-1906.

Ford, G.D., Ford, B.D., Steele, E.C. Jr., Gates, A., Hood, D., Matthews, M.A., Mirza, S., and Macleish, P.R. (2008). Analysis of transcriptional profiles and functional clustering of global cerebellar gene expression in PCD3J mice. Biochem. Biophys. Res. Commun. *377*, 556-561.

Fox, T.O. (1977). Estradiol and testosterone binding in normal and mutant mouse cerebellum: biochemical and cellular specificity. Brain Res. *128*, 263-273.

Greer, C.A., and Shepherd, G.M. (1982). Mitral cell degeneration and sensory function in the neurological mutant mouse Purkinje cell degeneration (PCD). Brain Res. *235*, 156-161.

Handel, M.A., and Dawson, M. (1981). Effects on Spermiogenesis in the mouse of a male sterile neurological mutant, purkinje cell degeneration. Gamete Res. *4*, 185-192.

Harris, A., Morgan, J.I., Pecot, M., Soumare, A., Osborne, A., and Soares, H.D. (2000). Regenerating motor neurons express Nna1, a novel ATP/GTP-binding protein related to zinc carboxypeptidases. Mol. Cell. Neurosci. *16*, 578-596.

Irizarry, R.A., Hobbs, B., Collin, F., Beazer-Barclay, Y.D., Antonellis, K.J., Scherf, U., and Speed, T.P. (2003). Exploration, normalization, and summaries of high density oligonucleotide array probe level data. Biostatistics *4*, 249-264.

Kalinina, E., Biswas, R., Berezniuk, I., Hermoso, A., Aviles, F.X., and Fricker, L.D. (2007). A novel subfamily of mouse cytosolic carboxypeptidases. FASEB J. *21*, 836-850.

Khatchadourian, K., Smith, C.E., Metzler, M., Gregory, M., Hayden, M.R., Cyr, D.G., and Hermo, L. (2007). Structural abnormalities in spermatids together with reduced sperm counts and motility underlie the reproductive defect in HIP1-/- mice. Mol. Reprod. Dev. *74*, 341-359.

Krulewski, T.F., Neumann, P.E., and Gordon, J.W. (1989). Insertional mutation in a transgenic mouse allelic with Purkinje cell degeneration. Proc. Natl. Acad. Sci. USA *86*, 3709-3712.

Kyuhou, S., Kato, N., and Gemba, H. (2006). Emergence of endoplasmic reticulum stress and activated microglia in Purkinje cell degeneration mice. Neurosci. Lett. *396*, 91-96.

Landis, S.C., and Mullen, R.J. (1978). The development and degeneration of Purkinje cells in pcd mutant mice. J. Comp. Neurol. *177*, 125-143.

LaVail, M.M., Blanks, J.C., and Mullen, R.J. (1982). Retinal degeneration in the pcd cerebellar mutant mouse. Ⅰ. Light microscopic and autoradiographic analysis. J. Comp. Neurol. *212*, 217-230.

Lee, K.H., Song, G.J., Kang, I.S., Kim, S.W., Paick, J.S., Chung, C.H., and Rhee, K. (2003). Ubiquitin-specific protease activity of USP9Y, a male infertility gene on the Y chromosome. Reprod. Fertil. Dev. *15*, 129-133.

Liu, D., Matzuk, M.M., Sung, W.K., Guo, Q., Wang, P., and Wolgemuth, D.J. (1998). Cyclin A1 is required for meiosis in the male mouse. Nat. Genet. *20*, 377-380.

Lok, S., Johnston, D.S., Conklin, D., Lofton-Day, C.E., Adams, R.L., Jelmberg, A.C., Whitmore, T.E., Schrader, S., Griswold, M.D., and Jaspers, S.R. (2000). Identification of INSL6, a new member of the insulin family that is expressed in the testis of the human and rat. Biol. Reprod. *62*, 1593-1599.

Ma, X., Dong, Y., Matzuk, M.M., and Kumar, T.R. (2004). Targeted disruption of luteinizing hormone beta-subunit leads to hypogonadism, defects in gonadal steroidogenesis, and infertility. Proc. Natl. Acad. Sci. USA *101*, 17294-17299.

McCleland, M.L., Farrell, J.A., and O'Farrell, P.H. (2009). Influence of cyclin type and dose on mitotic entry and progression in the early Drosophila embryo. J. Cell Biol. *184*, 639-46.

Mullen, R.J., Eicher, E.M., and Sidman, R.L. (1976). Purkinje cell degeneration, a new neurological mutation in the mouse. Proc. Natl. Acad. Sci. USA *73*, 208-212.

Nagamine, C.M., Chan, K., Hake, L.E., and Lau, Y.F. (1990). The two candidate testis-determining Y genes (Zfy-1 and Zfy-2) are differentially expressed in fetal and adult mouse tissues. Genes Dev. *4*, 63-74.

Nguyen, T.B., Manova, K., Capodieci, P., Lindon, C., Bottega, S., Wang, X.Y., Refik-Rogers, J., Pines, J., Wolgemuth, D.J., and Koff, J. (2002). Characterization and expression of mammalian cyclin b3, a prepachytene meiotic cyclin. J. Biol. Chem. *277*, 41960-41969.

O'Gorman, S. (1985). Degeneration of thalamic neurons in "Purkinje cell degeneration" mutant mice. II. Cytology of neuron loss. J. Comp. Neurol. *234*, 298-316.

O'Gorman, S., and Sidman, R.L. (1985). Degeneration of thalamic neurons in "Purkinje cell degeneration" mutant mouse. I. Distribution of neuron loss. J. Comp. Neurol. *234*, 277-297.

O'Shaughnessy, P.J., Monteiro, A., Verhoeven, G., De Gendt, K., and Abel, M.H. (2010). Effect of FSH on testicular morphology and spermatogenesis in gonadotrophin-deficienthypogonadal mice lacking androgen receptors. Reproduction *139*, 177-184.

Refik-Rogers, J., Manova, K., and Koff, A. (2006). Misexpression of cyclin B3 leads to aberrant spermatogenesis. Cell Cycle *5*, 1966-1973.

Robb, G.W., Amann, R.P., and Killian, G.J. (1978). Daily sperm production and epididymal sperm reserves of pubertal and adult rats. J. Reprod. Fertil. *54*, 103-107.

Rodriguez de la Vega, M., Sevilla, R.G., Hermoso, A., Lorenzo, J., Tanco, S., Diez, A., Fricker, L.D., Bautista, J.M., and Aviles, F.X. (2007). Nna1-like proteins are active metallocarboxypeptidases of a new and diverse M14 subfamily. FASEB J. *21*, 851-865.

Rong, Y., Wang, T., and Morgan, J.I. (2004). Identification of candidate Purkinje cell-specific markers by gene expression profiling in wild-type and pcd (3J) mice. Brain Res. Mol. Brain Res. *132*, 128-145.

Sun, Y.J., Nishikawa, K., Yuda, H., Wang, Y.L., Osaka, H., Fukazawa, N., Naito, A., Kudo, Y., Wada, K., and Aoki, S. (2006). Solo/Trio8, a membrane-associated short isoform of Trio, modulates endosome dynamics and neurite elongation. Mol. Cell. Biol. *26*, 6923-6935.

Sutovsky, P. (2003). Ubiquitin-dependent proteolysis in mammalian spermatogenesis, fertilization, and sperm quality control: killing three birds with one stone. Microsc. Res. Tech. *61*, 88-102.

Wang, T., and Morgan, J.I. (2007). The Purkinje cell degeneration (pcd) mouse: an unexpected molecular link between neuronal degeneration and regeneration. Brain Res. *1140*, 26-40.

Wang, T., Parris, J., Li, L., and Morgan, J.I. (2006). The carboxypeptidase-like substrate-binding site in Nna1 is essential for the rescue of the Purkinje cell degeneration (pcd) phenotype. Mol. Cell. Neurosci. *33*, 200-213.

Wu, L., Niemeyer, B., Colley, N., Socolich, M., and Zuker, C.S. (1995). Regulation of PLC-mediated signaling *in vivo* by CDP-diacylglycerol synthase. Nature *373*, 216-222.

Xiao, R., Park, Y., Dirisala, V.R., Zhang, Y.P., Um, S.J., Lee, H.T., and Park, C. (2005). Identification of genes differentially expressed in wild type and Purkinje cell degeneration mice. Mol. Cells *20*, 219-227.

Zachariae, W., Schwab, M., Nasmyth, K., and Seufert, W. (1998). Control of cyclin ubiquitination by CDK-regulated binding of Hct1 to the anaphase promoting complex. Science *282*, 1721-1724.

Zambrowicz, B.P., Zimmermann, J.W., Harendza, C.J., Simpson, E.M., Page, D.C., Brinster, R.L., and Palmiter, R.D. (1994). Expression of a mouse Zfy-1/lacZ transgene in the somatic cells of the embryonic gonad and germ cells of the adult testis. Development *120*, 1549-1559.